Received: 5 August 2021 | Revised: 22 January 2022 | Accepted: 13 February 2022

DOI: 10.1111/vsu.13798

ORIGINAL ARTICLE - RESEARCH

WILEY

Ex vivo comparison of 3 Tesla magnetic resonance imaging and multidetector computed tomography arthrography to identify artificial soft tissue lesions in equine stifles

Anton D. Aßmann MedVet[1] | Stefanie Ohlerth Prof, DrMedVet, DECVDI[2] | José Suárez Sánchez-Andráde, DVM, PhD, DECVDI[2] | Paul R. Torgerson Prof, VetMB, PhD, DECVPH, DEVPC[3] | Andrea S. Bischofberger PD, DrMedVet, PhD, DACVS, DECVS[1]

[1]Equine Hospital, Vetsuisse-Faculty, University of Zurich, Zurich, Switzerland

[2]Diagnostic Imaging Clinic, University of Zurich, Zurich, Switzerland

[3]Section of Veterinary Epidemiology, Vetsuisse-Faculty, University of Zurich, Zurich, Switzerland

Correspondence
Andrea Bischofberger, Equine Hospital, Vetsuisse-Faculty, University of Zürich, Winterthurerstrasse 260, 8057 Zürich, Switzerland.
Email: abischofberger@vetclinics.uzh.ch

Funding information
The study was funded by the Loriot Research Fund.

Abstract

OBJECTIVE: To determine the diagnostic performance of computed tomographic arthrography (CTA) and 3 Tesla magnetic resonance imaging (MRI) for detecting artificial meniscal, meniscotibial ligament (MTL) lesions and cruciate ligament (CL) lesions in horses.

STUDY DESIGN: Ex vivo controlled laboratory study.

ANIMALS: Nineteen stifles from adult horses.

METHODS: Stablike defects ($n = 84$) (16 mm long, 10 mm deep) were created in the menisci ($n = 35$), CLs ($n = 24$), and MTLs ($n = 25$) via arthroscopy prior to MRI and CTA (80 mL contrast at 85 mg/mL per joint). Two radiologists, unaware of the lesions, reached a consensus regarding the presence of lesions, based on 2 reviews of each study. Sensitivity and specificity of MRI and CTA were determined using arthroscopy as a reference and compared with McNemar's tests.

RESULTS: The sensitivity and specificity of MRI (41% and 86% respectively) and CTA (32% and 90% respectively) did not differ ($P = .65$). The sensitivity (MRI: 24%-50%; CTA:19%-40%) and specificity (MRI: 75%-92%; CTA 75%-100%) of imaging modalities did not differ when detecting lesions of the menisci, MTLs, and CLs ($P = .1$-1.0). The highest sensitivities were achieved when MTLs were evaluated with MRI (50%) and CLs with both modalities (40%).

CONCLUSIONS: The diagnostic performance of CTA was comparable with that of MRI, with a low to moderate sensitivity and high specificity.

CLINICAL SIGNIFICANCE: Computed tomographic arthrography should be considered as an adjunct to diagnose CL injuries. This is important for equine clinicians, as the CL cannot be visualized adequately using basic imaging techniques preoperatively.

This is an open access article under the terms of the Creative Commons Attribution-NonCommercial-NoDerivs License, which permits use and distribution in any medium, provided the original work is properly cited, the use is non-commercial and no modifications or adaptations are made.
© 2022 The Authors. *Veterinary Surgery* published by Wiley Periodicals LLC on behalf of American College of Veterinary Surgeons.

1 | INTRODUCTION

Hind limb lameness due to stifle joint pathologies are common in sport horses.[1–3] Injuries of the subchondral bone, cartilage, and soft tissues, including the cruciate ligaments, the menisci, and the meniscotibial ligaments, often represent the underlying cause of pain. Meniscal lesions represent up to 68% of soft tissue lesions in the stifle, whereas cruciate ligament lesions only account for 9%.[4] Meniscal lesions vary in their severity and are graded from tears in the meniscus without significant separation (grade I), over complete tears in the cranial pole of the meniscus (grade II), to severe tears of the meniscus, which extend beneath the femoral condyle (grade III).[5] Although they are rare in horses, cranial cruciate ligament injury is far more common than caudal cruciate ligament injury.[6–8] Partial or complete tearing of the cranial cruciate ligament most commonly occurs in the midbody.[8,9]

Advanced imaging may be available to some readers but a sound understanding of basic imaging techniques is more generally transferable. Radiography may only be useful for the diagnosis of soft tissue lesions in the stifle if mineralization of soft tissue structures, enthesiophyte formation, or avulsion fractures are present.[10,11] Ultrasonography is limited in the ability to appropriately visualize all soft tissue structures within the stifle. Meniscal lesions have been identified considerably more often by ultrasonography than by arthroscopy[12–14] but meniscotibial ligament and cruciate ligament lesions have been better detected by arthroscopy.[12] In one study, 14 out of 25 cases were diagnosed with a meniscotibial ligament tear by arthroscopy, whereas only 5 tears were diagnosed with ultrasonography.[14] Adrian et al. demonstrated a significantly higher difference diagnosing meniscotibial tears by arthroscopy than by ultrasonography.[12] Cruciate ligaments can only be poorly and partially visualized using ultrasonography.[12,15] It has therefore been recommended that basic imaging techniques, such as ultrasonography, are used in conjunction with arthroscopy, when diagnosing stifle pathologies.[16]

Arthroscopic exploration under general anesthesia represents the gold standard to diagnose stifle joint pathologies.[14,17] A standing method for use in appropriate cases, using a needle arthroscope, has also been described.[18] Independent of the technique used, only a third of the menisci and the cruciate ligaments can be visualized. In addition, examination of the opposing articular cartilage is impaired.[18–20] A noninvasive preoperative diagnostic imaging tool, allowing complete examination of the stifle joint, would therefore be the instrument of choice.

Nowadays, magnetic resonance imaging (MRI) is an integral part of the examination of knee disorders in humans and small animals.[21] Because of its excellent soft-tissue detail and contrast resolution, MRI is considered a leading noninvasive diagnostic imaging modality for soft-tissue abnormalities in the horse.[22–24] Unfortunately, scanning the equine stifle joint with high-field magnets is greatly limited due to magnet bore diameter, hindering the implementation of MRI as the standard diagnostic imaging modality in horses to diagnose stifle disease.[25] So far, stifle pathologies using a low field MRI system and the normal high-field MRI appearance of soft tissue structures in the equine stifle have been reported.[26–28] However, the diagnostic performance of low-field MRI has not yet been investigated.

Computed tomography (CT) is limited in the visualization of soft tissue structures unless intravenous, intra-arterial, and/or intra-articular contrast medium is added.[29] Intra-articular contrast medium diffuses within the joint, outlining intra-articular soft tissue structures and articular cartilage. Consequently, abnormalities in size, shape, or contours of the intrasynovial tissues may be identified.[30] In humans suffering from claustrophobia and patients with subcutaneous defibrillators or other ferromagnetic implants, where MRI is contraindicated, multidetector computed tomographic arthrography (CTA) of the stifle is used alternatively.[31,32] In the human knee, CTA is effective with a reported sensitivity and specificity of 98% and 94%, 90%, and 96%, respectively, for meniscal and cranial cruciate ligament injuries.[33–36] CTA is also being performed in larger equine clinics and the normal CTA anatomy of the stifle joint and its use for the diagnosis of disease entities have been reported.[14,30,37–39] No studies comparing high-field MRI with CTA in the ability to detect soft tissue lesions in the stifle have been published yet.

The objective of this study was to determine the diagnostic performance of CTA and 3 Tesla MRI for detecting artificial meniscal, meniscotibial ligament- and cruciate ligament lesions in horses. We hypothesized that CTA and high-field MRI would have a similar diagnostic performance in diagnosing artificially created lesions in each of 7 clinically relevant locations within the stifle (menisci, meniscotibial ligaments, cranial, and caudal cruciate ligaments).

2 | MATERIALS AND METHODS

2.1 | Specimen collection

Within 24 hours after euthanasia, 19 stifle joints were collected from Warmblood and Thoroughbred horses, aged 5-22 years old, of mixed-sex, euthanized for reasons unrelated to the musculoskeletal apparatus. Following

owner consent, the stifles were removed by disarticulation in the coxofemoral joint, serially numbered, and stored at −28 °C. Experimental subjects were thawed underwater until they reached room temperature and then prepared for stifle joint arthroscopy.

2.2 | Arthroscopy of the stifle

Each limb was fixed on a table and the foot attached to a hoist, to allow limb flexion and extension during arthroscopy. A board-certified surgeon (AB, AA) performed all arthroscopies, using a 30° forward angled, 4 mm rigid arthroscope. The medial compartment of the femorotibial joint was examined via a cranial and caudal approach, whereas the lateral compartment was approached cranially only. Briefly, the stifle was flexed at 90° for the cranial approach. A skin incision was made with a No. 11 surgical scalpel blade and continued through the fascia into the middle patellar ligament, about 2 cm proximal to the tibial crest. The arthroscopic sleeve containing the conical obturator was inserted in a slightly proximad, caudad, and axial direction until it penetrated the medial femorotibial joint capsule. The arthroscopic sleeve, containing the conical obturator, was pulled back without leaving the incision into the middle patellar ligament and directed in the same fashion as before, to enter the lateral femorotibial joint.

The stifles were extended to 120° flexion, to access the caudal part of the medial femorotibial joint. Then the scope was pushed via the cranial approach abaxially as far as possible to the caudal side, to improve the joint distention caudally. The arthroscopic portal was made about 6-8 cm caudal to the medial collateral ligament, 1 cm proximal to the level of the line between the palpable tibial tuberosity and tibial condyle, 1-2 cm cranial to the medial saphenous vein.[17]

First, the stifle joint compartments were examined for pre-existing lesions of the menisci, meniscotibial, and cruciate ligaments. Only arthroscopically normal stifles were included in the study. A lesion was made in the cranial meniscotibial ligament, the cranial as well as the caudal horn of the medial meniscus, and/or the caudal cruciate ligament within the medial femorotibial joint. In the cranial part of the lateral femorotibial joint, a lesion was made in the cranial meniscotibial ligament, the cranial horn of the lateral meniscus, and/or the cranial cruciate ligament. Figures 1–3 show the lesions made in the cruciate ligament, the meniscotibial ligament, and the meniscus. Lesions were created, using an arthroscopic scalpel (blade dimensions: 16 mm long and 5 mm wide). Lesion length and depth were standardized to 16 mm and 10 mm, respectively, based on the dimensions of the arthroscopic scalpel used. Every ligament lesion was made by stabbing into the ligament parallel to its fiber course, over a length of 10 mm. Once the cut was made, the scalpel blade was turned more transversely and obliquely to widen the split carefully, and fray the ligament fibers superficially, without cutting perpendicular to the fiber course through the structures when doing so. This resulted in small partial lesions and fiber tearing parallel to the fiber course of the respective structure. A cruciate ligament lesion was placed approximately in its midbody. Meniscal lesions were made horizontally in the cranial and caudal meniscal horn, mimicking horizontal transverse tears of grade I in a similar fashion as described above. Hence, in 17 stifles, a maximum of 119 lesions would have been possible. However, only 84 lesions were created, leaving 16 menisci, 9 meniscotibial, and 10 cruciate ligaments intact to serve as controls. All arthroscopic portals were closed in a standard fashion in 2 layers including the joint capsule and the skin. Following arthroscopy, all limbs were frozen at −28 °C.

2.3 | Imaging studies

All limbs were thawed for 24 h before MRI was performed at room temperature with a 3 Tesla MRI scanner and a dStream Torso coil (Philips Ingenia, Philips AG, Zurich, Switzerland). Limbs were positioned in lateral recumbency, with the toe facing away from the gantry. Magnetic resonance imaging sequences, planes, and acquisition parameters are summarized in Table 1.

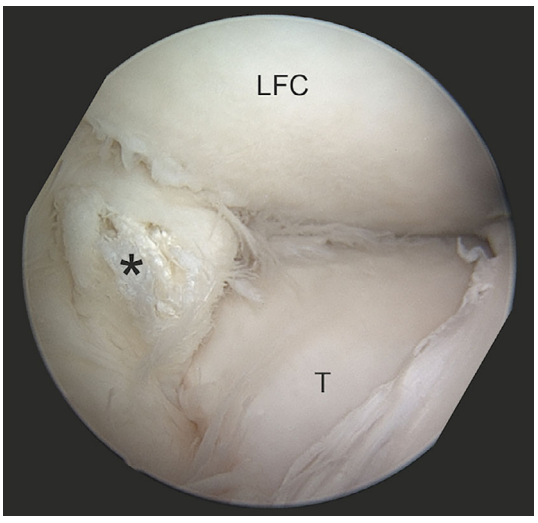

FIGURE 1 Arthroscopic image of an experimental lesion created in the cranial cruciate ligament (asterisk) via a cranial approach to the lateral femorotibial joint. Abbreviations: LFC, lateral femoral condyle; T, lateral tibial condyle

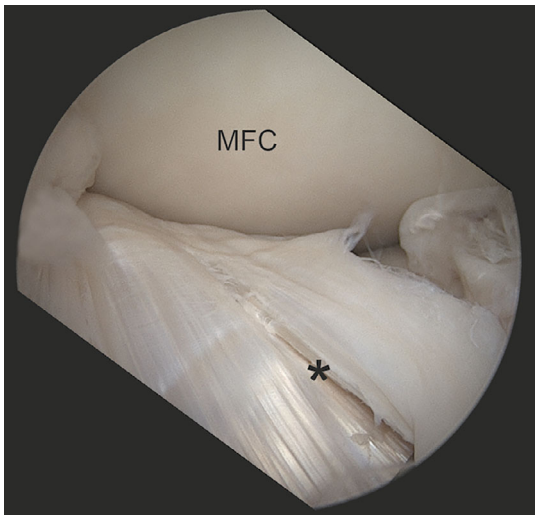

FIGURE 2 Arthroscopic image of an experimental lesion created in the medial cranial meniscotibial ligament (asterisk) via a cranial approach to the medial femorotibial joint. Abbreviation: MFC, medial femoral condyle

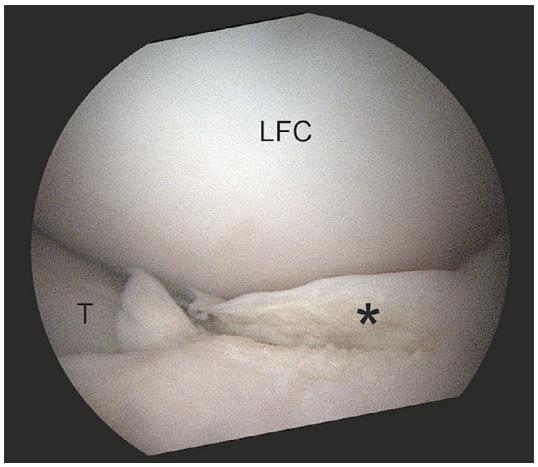

FIGURE 3 Arthroscopic image of an experimental lesion created in the cranial horn of the lateral meniscus (asterisk) via a cranial approach to the lateral femorotibial joint. Abbreviations: LFC, lateral femoral condyle; T, lateral tibial condyle

Subsequently, each femorotibial joint compartment was injected with 80 mL iodinated contrast medium with 350 mg Iodine/ml (Optiray 350, Mallinckrodt AG, Steinhausen, Switzerland), diluted 1:4 with 0.9% NaCl, to gain a concentration of 85 mg/mL.[30] The lateral femorotibial joint was injected by inserting a 20 gauge, 70 mm long needle caudal to the lateral patellar ligament, just above the proximolateral edge of the tibia plateau. The medial femorotibial joint was injected by inserting a 20 gauge, 70 mm long needle between the medial patellar ligament and the medial collateral ligament, just above the proximomedial edge of the tibia

TABLE 1 Magnetic resonance imaging sequences and parameters used in the present study

Sequence	T2W_TSE_Sag	T2W_TSE_Cor	T2W_TSE_Tra	3D_T2W_HR	3D_PDW_SPAIR	T2_3D_mFFE	T1W_VISTA_SPAIR
TR	4557	4674	3737	1300	1200	31	350
TE	80	80	80	257	194	9.2	19
Flip angle	90	90	90	90	90	90	90
Echo train length	14	12	20	85	42	3	24
NEX	1	1	1	1	1	1	1
FOV	250 × 250 × 181 mm	230 × 202 × 188 mm	220 × 220 × 221 mm	220 × 202 × 300 mm	200 × 250 × 300 mm	200 × 200 × 300 mm	250 × 199 × 300 mm
Frequency direction	FH	RL	RL	AP	FH	AP	AP
Fat suppressed	No	No	No	No	No	No	No
Slice thickness	3 mm	3 mm	3 mm	0.55 mm	0.7 mm	2 mm	0.7 mm
Gap width	3 mm	3 mm	3 mm	−0.3 mm	0 mm	−1 mm	−0.35 mm
Number of slices	55	57	67	382	286	200	571
Time to run (min)	7.45	6.13	6.14	8.28	7.52	5.46	7.46

Abbreviations: NEX, Number of excitations; FOV, field of view; TE, time to echo; TR, time to repeat.

plateau.[40] Following injection of the contrast medium each limb was flexed and extended for 2 minutes to ensure even contrast distribution within the joint. Within 20 minutes after contrast injection, CT images were obtained, using a multidetector 16 slice scanner (Philips 16 Brilliance, Philips AG, Zurich, Switzerland) in helical mode acquisition, with a pitch of 0.55, 140 kV, 350 mAs, a field of view of 176 mm, a matrix of 3000 × 300. Images were reconstructed in a bone and soft tissue algorithm with a slice thickness of 0.6 mm.

2.4 | Evaluation of imaging studies

Using a diagnostic workstation and medical imaging software (Intellispace PACS Radiology 4.4553.0, Phillips Healthcare, Zurich, Switzerland), 2 board-certified radiologists (SO and JSS) reviewed all images twice and individually. In cases, with divergent results, a consensus was reached. Stifles had to be reviewed by each radiologist in a randomly generated order. Observers were unaware of the presence, location, severity, and the total number of joint lesions. Images were examined in all planes and using multiplanar reconstruction for the presence or absence of lesions in the aforementioned soft tissue structures in the femorotibial joint (MRI diagnosis, CTA diagnosis: no lesion, lesion present). The definition of the normal CTA and MRI appearance of the investigated soft tissue structures was based on the current literature.[28,37,41] A lesion was considered present in a meniscotibial ligament (1) if synovial fluid/contrast medium was infiltrating with focal internal signal/contrast accumulation or (2) if in MRI, partial or complete truncation with loose fibers was noted, or (3) in CTA, abnormal or unclear margins were identified. In the menisci, a lesion was present (1) if synovial fluid/contrast medium was infiltrating with a linear or focal internal signal/contrast accumulation and/or a meniscal fragment was seen, or (2) abnormal margins were noted. A lesion was considered present in the cruciate ligaments with either modality (1) if synovial fluid/contrast medium was infiltrating with focal internal signal/contrast accumulation, or (2) an abnormal shape (marked focal thickening, bowed, or undulating contours) was noted.

2.5 | Statistical analysis

Data were stored in Microsoft Excel. The distribution of data for continuous variables was assessed for normality by use of the Kolmogorov-Smirnoff test. Results were reported as the mean ± standard deviation for variables with parametric distribution and median (range) for variables with nonparametric distributions.

The diagnostic performance of MRI and CTA (sensitivity, specificity) was calculated for all lesions independent of the affected structure and lesion groups (both meniscotibial ligaments, both menisci, both cruciate ligaments). Arthroscopy served as the gold standard. Sensitivities and specificities between both modalities were compared using McNemar's tests. Binary logistic regression was used to evaluate the association of the independent variable sex and the covariate age on MRI or CTA diagnosis (no lesion, lesion present). All statistical analyses were performed with commercially available statistical software programs (R Core Team [2016]. R: A language and environment for statistical computing. R Foundation for Statistical Computing, Vienna, Austria. URL https://www.R-project.org/.) using the MASS, car and lme4 packages and SPSS Inc, Chicago, Illinois) and a P-value <.05 was considered significant.

3 | RESULTS

Nineteen hindlimbs (9 left and 10 right limbs) of 11 warmblood cadaver horses (6 mares and 5 geldings), with a mean age of 14.2 ± 4.85 years (5-22 years), were obtained and underwent stifle arthroscopy. Due to preexisting pathological changes within 2 stifle joints (1 meniscal lesion, 1 osteoarthritis), these stifle specimens

TABLE 2 Sensitivity and specificity of magnetic resonance imaging (MRI) and computed tomography arthrography (CTA) to detect experimental lesions in different soft tissue structures of the equine stifle as well as results of McNemar's tests for the comparison of sensitivities and specificities between magnetic resonance imaging (MRI) and computed tomography arthrography (CTA)

Lesion	*P*-value	Sensitivity(%) (95% CI), (n)	*P*-value	Specificity(%) (95% CI), (n)
MRI meniscotibial ligament	0.45	50% (27%–73%), (10)	1	75% (35%–97%), (6)
CTA meniscotibial ligament		30% (12%–54%), (6)		75% (35%–97%), (6)
MRI meniscus	0.1	24% (12%–39%), (10)	1	92% (64%-99%), (12)
CTA meniscus		19% (9%-34%), (8)		100% (75%-100%), (13)
MRI cruciate ligaments	1	40% (19%-64%), (8)	1	87.5% (47%-99%), (7)
CTA cruciate ligaments		40% (19%-64%), (8)		87.5% (47%-99%), (7)

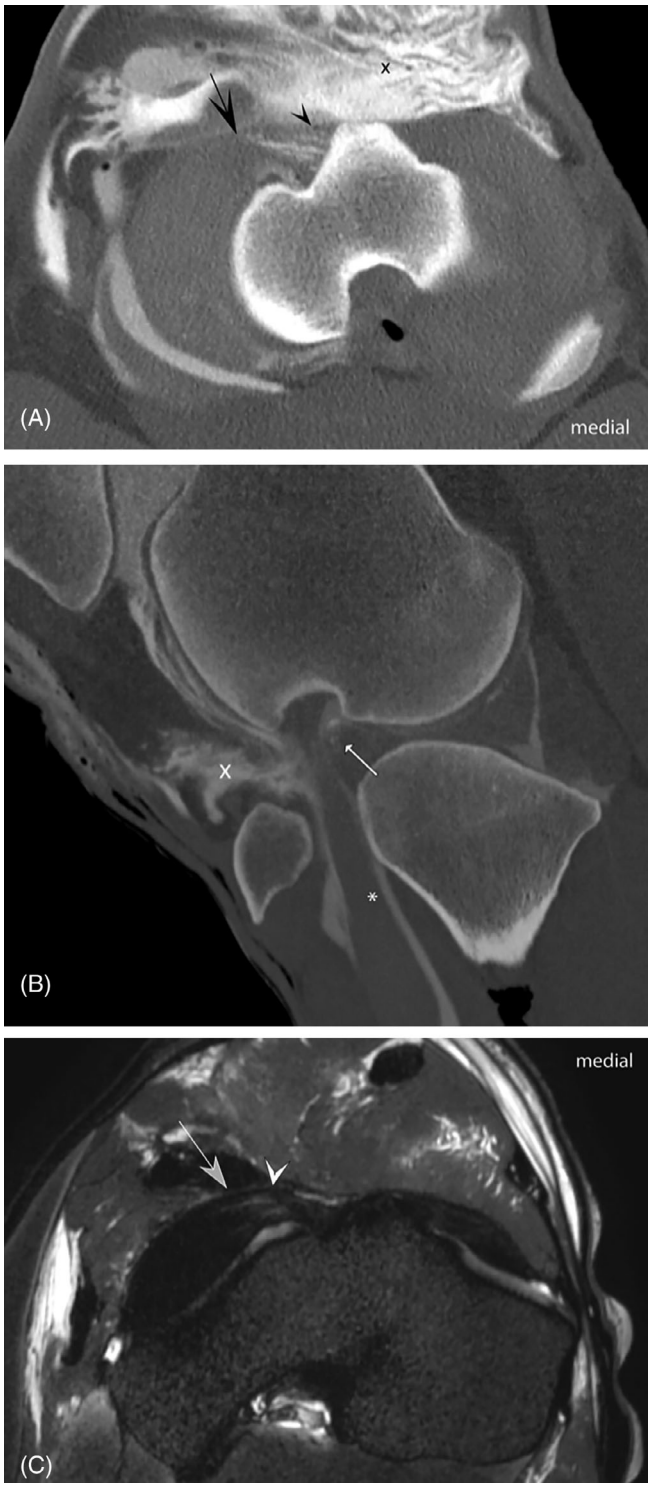

FIGURE 4 Images A (transverse computed tomographic image), B (sagittal plane computed tomographic image) and C (3D-T2-weighted high-resolution dorsal plane magnetic resonance image) showing a true positive lesion in the cranial meniscotibial ligament (arrowhead) and cranial horn of the lateral meniscus (arrow) in a cadaveric equine stifle. There is a clear linear infiltration of contrast medium/synovial fluid.
Note the extravasation of contrast medium/synovial fluid cranial and lateral to the femorotibial joint (x). The long digital extensor tendon is marked by the asterisk

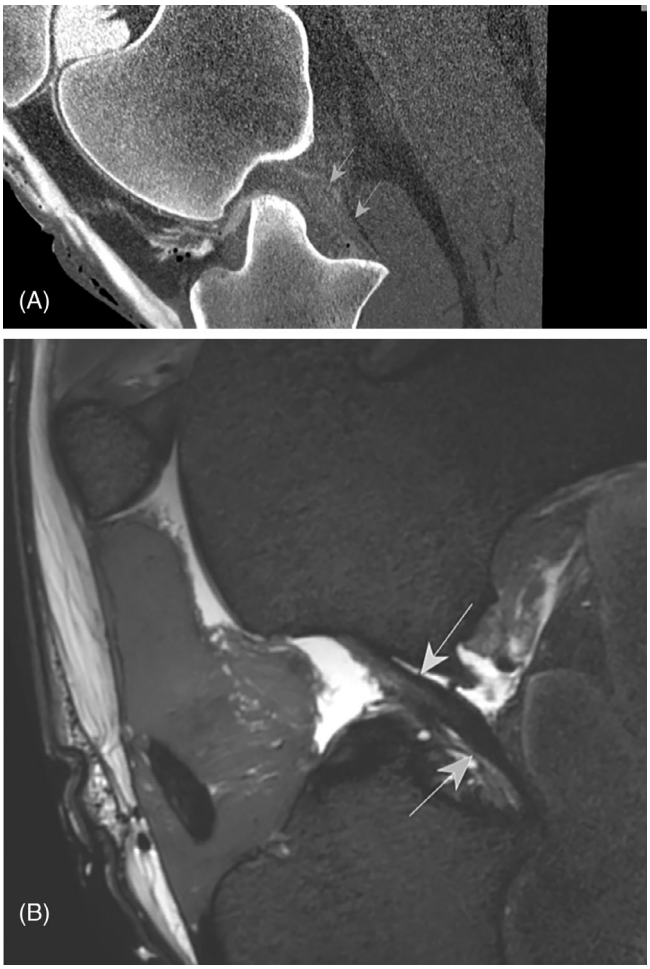

FIGURE 5 Images A (sagittal computed tomographic (CT) image) and B (corresponding T2-weighted high-resolution magnetic resonance image (MRI) show a true positive lesion in the caudal cruciate ligament in a cadaveric equine stifle. The caudal cruciate ligament is faintly outlined with contrast medium on CT and shows an abnormal shape with a bulging midportion and thinner distal portion with both modalities (arrows). With CT, the midportion appears mildly hyperdense and, with MRI, an increased signal intensity with mild linear infiltration is seen. The proximal portion is not well delineated on CT and the borders appear mildly irregular on MRI

were excluded from the study. Accordingly, a total of 84 lesions were created in the medial ($n = 49$) and/or lateral ($n = 35$) compartment of the femorotibial joints.

The quality of the MRI studies was considered good to excellent in all stifles by both reviewers. Reviewers did not feel that the intraarticular air in consequence of arthroscopy impaired the visibility of the structures to be evaluated. However, the quality of the CTA studies was considered inferior in 3 joints due to the nonuniform distribution of the contrast medium. These joints were excluded from the statistical analysis. With both modalities, mild to moderate extravasation of synovial fluid/

contrast medium was observed in all stifles along the arthroscopic portals.

Age and sex were not associated with MRI or CTA diagnosis ($P = .05$-1.0). For all lesions and both modalities (MRI, CTA), the overall sensitivity was low, whereas specificity was good. The sensitivity of MRI was similar (41%), compared to CTA (32%). Likewise, specificity values were comparable (MRI, 86%; CTA, 90%). Consequently, the diagnostic performance of MRI and CTA did not differ ($P = .65$).

For the different lesion groups (menisci, meniscotibial ligaments, cruciate ligaments), true positive rates of both modalities were low to moderate (MRI: 24%-50%; CTA:19%-40%), whereas true negative rates were good to excellent (MRI: 75-92%; CTA 75%-100%) (Table 2). In general, the performance of MRI was similar to CTA in diagnosing lesions in the meniscotibial ligaments, menisci, and cruciate ligaments (true positives) (Figures 4 and 5). Likewise, MRI and CTA had a similar performance in identifying normal meniscotibial ligaments, menisci, and cruciate ligaments (true negatives) ($P = 1.0$) (Table 2).

4 | DISCUSSION

Injuries of the soft tissue structures of the equine stifle are common and clinically relevant. With the increasing availability of CT and the limited access to MRI, CTA is nowadays commonly performed by equine specialists. Since MRI is considered the gold standard for the diagnosis of lesions in the soft tissue structures of the stifle in humans and canines, the goal of the present study was to determine the diagnostic performance of CTA in comparison to high-field MRI in an experimental setting. The authors of the present investigation hypothesized that diagnostic performance of CTA and high-field MRI would be similar for the detection of artificial meniscal, meniscotibial ligament, cranial, and caudal cruciate ligament lesions within the stifle. This assumption was the case for all lesions and the lesion groups, considering the diagnostic performance of both modalities did not differ.

Since the cruciate ligament lesions of the present study represented partial tears, sensitivity and specificity values were similar to, but in the lower range of reported values for MRI in the human knee with incomplete anterior cruciate ligament tears.[21,42–45] The diagnostic performance of CTA for anterior cruciate ligament tears in humans is excellent; however, most studies do not differentiate between complete and partial tears.[33] In dogs, CTA was also able to achieve high sensitivity values of 96%-100% and specificity values of 75%-100% for cranial cruciate ligament lesions (partial and complete tears).[46] So far, one report has compared CTA to arthroscopy in the equine stifle.[14] Detection rate of cranial meniscotibial ligament injuries was high with CTA (11 of 14 defects), whereas only 1 out of 3 cruciate ligament defects was identified.[14] Nevertheless, CTA sensitivity was best for cruciate ligament lesions, which is promising for its use in clinical patients, as cruciate ligament disease is often difficult to impossible to diagnose preoperatively using conventional imaging techniques.

With both modalities, true positive rates were the lowest for meniscal lesions in the present study. This is in contrast to excellent values reported for the human knee in high-field MRI: if intrameniscal hyperintense signal breaching the articular surface is seen on 2 slices with a 3 mm slice thickness, the positive predictive values were 94%-96%. However, if this finding was present on a single slice only, the positive predictive value decreased to 18%-43%.[21] Since high-resolution 3D sequences were also applied in the present study, lesions with a length of 10 mm should have theoretically been identified. Still, studies in dogs also demonstrated rather low sensitivity values of 45%-90% for meniscal lesions as well as cranial cruciate ligament lesions in MRI.[47,48] Likewise, CTA reported sensitivity values of 13%-73% and specificity values of 57%-100% for meniscal lesions.[46]

Manifold reasons for the high false-negative rates and the few false-positive cases may have played a role in the present study. Lesions were artificial and aimed to mimic naturally occurring small partial lesions. In the specific case of the menisci, the placed lesions in our study mainly resembled type I lesions. These lesions were also often placed horizontally. These horizontal pathologies are of course a minority in the clinical spectrum of cases. Our created lesions are substantially smaller and understandably more difficult to detect than the lesions that may occur clinically. Lesions within the meniscotibial and cruciate ligaments were also parallel to their long axis. These lesions may have been missed with both modalities because they were mistaken as the normal longitudinal striations of these ligaments. In all soft-tissue structures, the lesions may have collapsed due to lack of synovial effusion, impairing infiltration of synovial fluid/contrast medium. Furthermore, in contrast to clinical cases, lesions were rather small and reviewers could not take all MRI or CTA criteria into account. The obvious increased internal signal intensity of the ligaments and menisci, the abnormal underlying bone or periligamentous changes, and meniscal abnormalities such as abnormal margins/shape, presence of adipose/fibrous tissue, or meniscal-capsular dissociation, could have helped detect lesions. In MRI, magic angle artifacts within the soft structures may have obscured smaller lesions.[28]

Due to the experimental design, arthroscopy preceded diagnostic imaging and therefore, the femorotibial joint capsule was perforated and damage to the median septum, between the medial and lateral femorotibial joints, may have occurred due to the creation of the lesions. This caused a certain amount of leakage of intra-articular fluid or contrast into the periarticular tissues and resulted in uneven distribution of intra-articular fluid and a decreased concentration of the contrast medium. Likewise, the intra-articular pressure may have been lowered impairing the infiltration of lesions, in particular in the cranial aspects of the femorotibial joints. However, this issue should be limited to the cadaver study and better results regarding contrast filling and distribution can be expected in clinical cases. In our study, a contrast medium concentration in the range previously described was used at the lower range, however.[30] No studies have yet investigated the optimal contrast volume and concentration needed to detect soft tissue lesions within the femorotibial joints. It can only be postulated that a higher contrast concentration in combination with a larger volume might have resulted in a better lesion detection rate.

True negative rates were good to excellent in the present study. Both modalities appear highly accurate for the diagnosis of a normal, ie intact soft tissue structure in the equine stifle.

The range of confidence intervals was very wide for the data set of our study. This is, on one hand, caused by the experimental design of the study and on the other hand, by the number of cadaver joints used. Nevertheless, even with the low number of cadaver joints studied, the sensitivity and specificity values of the diagnostic imaging procedures should be sufficiently high to make them useful and accurate tools in a clinical setting.

In conclusion, CTA performed similarly to high-field MRI in detecting experimentally created soft tissue lesions in the stifle joint. CTA sensitivity was best for cruciate ligament lesions, which is important for equine clinicians as this ligament cannot be visualized adequately using basic imaging techniques. Computed tomographic arthrography was the least sensitive when diagnosing meniscal lesions. In these cases, adjunctive ultrasonographic examination of the menisci specifically may help increase the sensitivity of the overall preoperative diagnostic workup of stifle pathologies. Computed tomographic arthrography and MRI showed high specificity, thus being highly accurate in diagnosing an intact soft tissue structure. This is an important result for the future use of CTA in clinical cases, for instance when aiming at excluding certain soft tissue lesions within the stifle joint in horses without undergoing arthroscopy. Computed tomographic arthrography should be used in the preoperative diagnostic workup of stifle pathologies when ultrasonography is not definitive, or a cruciate ligament lesion is suspected.

ACKNOWLEDGMENTS

Author Contributions: Aßmann AD, MedVet: Conception and design of the study and data collection; analysis and interpretation of the data; writing the manuscript and revising it. Ohlerth S, Prof, DrMedVet, DECVDI: Conception and design of the study and data collection; analysis and interpretation of the data; writing the manuscript and revising it. Suárez Sánchez-Andráde J, DVM, PhD, ECVDI: Analysis and interpretation of the data. Torgerson PR, Prof, VetMB, DECVPH, DEVPC: Analysis and interpretation of the data; writing the manuscript and revising it. Bischofberger AS, PD, DrMedVet, PhD, DACVS, DECVS: Conception and design of the study and data collection; analysis and interpretation of the data; responsible for writing the manuscript and revising it.

All authors gave their final approval of the manuscript. All authors have made substantial contributions to the study.

We thank Nico Bolz for his contribution to the practical part of the study. Open access funding provided by Universitat Zurich.

CONFLICT OF INTERESTS

The authors declare no conflict of interest related to this report.

REFERENCES

1. Singer ER, Barnes J, Saxby F, Murray JK. Injuries in the event horse: training versus competition. *Vet J*. 2008;175:76-81.
2. Jeffcott L, Kold S. Stifle lameness in the horse: a survey of 86 referred cases. *Equine Vet J*. 1982;14:31-39.
3. Dyson SJ. Lameness associated with the stifle and pelvic regions. *Proc AAEP*. 2002;48.387-411.
4. Cohen JM, Richardson DW, McKnight AL, et al. Long-term outcome in 44 horses with stifle lameness after arthroscopic exploration and debridement. *Vet Surg*. 2009; 38:543-551.
5. Walmsley JP, Phillips TJ. Townsend: meniscal tears in horses: an evaluation of clinical signs and arthroscopic treatment of 80 cases. *Equine Vet J*. 2003;35:402-406.
6. Auer J, Stick JA, Kümmerle JM, Prange T. *Equine Surgery*. 5th ed. Elsevier; 2019:1759-1763.
7. Baker G, Moustafa M, Boero M, Foreman J, Wilson D. Caudal cruciate ligament function and injury in the horse. *Vet Rec*. 1987;121:319-321.
8. Walmsley JP. Diagnosis and treatment of ligamentous and meniscal injuries in the equine stifle. *Vet Clin Equine Pract*. 2005;21:651-672.
9. Rich FR, Glisson RR. In vitro mechanical properties and failure mode of the equine (pony) cranial cruciate ligament. *Vet Surg*. 1994;23:257-265.

10. Aldrich ED, Goodrich LR, Monahan MK, Conway JD, Valdés-Martinez A. Radiographic localisation of the entheses of the equine stifle. *Equine Vet J*. 2017;49:493-500.
11. Maulet BEB, Mayhew I, Jones E, Booth TH. Radiographic anatomy of the soft tissue attachments of the equine stifle. *Equine Vet J*. 2005;37:530-535.
12. Adrian AM, Barrett MF, Werpy NM, Kawcak CE, Chapman PL, Goodrich LR. A comparison of arthroscopy to ultrasonography for identification of pathology of the equine stifle. *Equine Vet J*. 2017;49:314-321.
13. Barr ED, Pinchbeck GL, Clegg PD, Singer ER. Accuracy of diagnostic techniques used in investigation of stifle lameness in horses-40 cases. *Equine Vet Educ*. 2006;18:326-332.
14. Nelson BB, Kawcak CE, Goodrich LR, Werpy NM, Valdés-Martinez A, Mcllwraith CW. Comparison between computed tomographic arthrography, radiography, ultrasonography, and arthroscopy for the diagnosis of femorotibial joint disease in western performance horses. *Vet Radiol Ultrasound*. 2016;387-402:387-402.
15. Penninck DG, Nyland TG, O'Brien TR, Wheat JD, Berry CR. Ultrasonography of the equine stifle. *Vet Radiol*. 1990;31:293-298.
16. Barrett MF, Frisbie DD, McIlwraith CW, Werpy NM. The arthroscopic and ultrasonographic boundaries of the equine femorotibial joints. *Equine Vet J*. 2012;44:57-63.
17. McIlwraith CW, Nixon AJ, Wright IM. *Diagnostic and Surgical Arthroscopy in the Horse*. 4th ed. Elsevier; 2014.
18. Frisbie DD, Barrett MF, McIlwraith CW, Ullmer J. Diagnostic stifle joint arthroscopy using a needle arthroscope in standing horses. *Vet Surg*. 2014;43:12-18.
19. Peroni JF, Stick JA. Evaluation of a cranial arthroscopic approach to the stifle joint for the treatment of femorotibial joint disease in horses: 23 cases (1998–1999). *J Am Vet Med Assoc*. 2002;220:1046-1052.
20. Watts AE, Nixon AJ. Comparison of arthroscopic approaches and accessible anatomic structures during arthroscopy of the caudal pouches of equine femorotibial joints. *Vet Surg*. 2006;35:219-226.
21. Nacey NC, Geeslin MG, Miller GW, Pierce J. Magnetic resonance imaging of the knee: an overview and update of conventional and state of the art imaging. *J Magn Reson Imaging*. 2017;45:1257-1275.
22. Dyson SJ, Murray R, Schramme MC. Lameness associated with foot pain: results of magnetic resonance imaging in 199 horses (January 2001–December 2003) and response to treatment. *Equine Vet J*. 2005;37:113-121.
23. Murray RC. *Equine MRI*. John Wiley & Sons; 2011.
24. Werpy NM, Denoix JM, McIlwraith CW, Frisbie DD. Comparison between standard ultrasonography, angle contrast ultrasonography, and magnetic resonance imaging characteristics of the normal equine proximal suspensory ligament. *Vet Radiol Ultrasound*. 2013;54:536-547.
25. Judy CE. Magnetic resonance imaging of the equine stifle in a clinical setting. *Proc ACVS*. 2007;36:163-166.
26. Waselau M, McKnight A, Kasparek A. Magnetic resonance imaging of equine stifles: technique and observations in 76 clinical cases. *Equine Vet Educ*. 2020;32:85-91.
27. McKnight AL. MRI of the equine stifle – 61 clinical cases. *J Equine Vet Sci*. 2012;10:672.
28. Daglish J, Frisbie DD, Selberg KT, Barrett MF. High field magnetic resonance imaging is comparable with gross anatomy for description of the normal appearance of soft tissues in the equine stifle. *Vet Radiol Ultrasound*. 2018;59:721-736.
29. Puchalski SM. Advances in equine computed tomography and use of contrast media. *Vet Clin North Am Equine Pract*. 2012;28:563-581.
30. Valdés-Martínez A. Computed tomographic arthrography of the equine stifle joint. *Vet Clin North Am Equine Pract*. 2012;28:583-598.
31. Hailey D. Open magnetic resonance imaging (MRI) scanners. *Issues Emerg Health Technol*. 2006;92:1-4.
32. Lee M-J, Kim S, Lee S-A, et al. Overcoming artifacts from metallic orthopedic implants at high-field-strength MR imaging and multi-detector CT. *Radiographics*. 2007;27:791-803.
33. De Filippo M, Bertellini A, Pogliacomi F, et al. Multidetector computed tomography arthrography of the knee: diagnostic accuracy and indications. *Eur J Radiol*. 2009;70:342-351.
34. Kalke RJ, Di Primio GA, Schweitzer ME. MR and CT arthrography of the knee. *Musculoskelet Radiol*. 2012;16(1):57-68.
35. Vande Berg BC, Lecouvet FE, Poilvache P, et al. Dual-detector spiral CT arthrography of the knee: accuracy for detection of meniscal abnormalities and unstable meniscal tears. *Radiology*. 2000;216:851-857.
36. Vande Berg BC, Lecouvet FE, Poilvache P, Dubuc JE, Maldaque B, Melghem J. Anterior cruciate ligament tears and associated meniscal lesions: assessment at dual-detector spiral CT arthrography. *Radiology*. 2002;223:403-409.
37. Van der Vekens E, Bergman EH, Vanderperren K, et al. Computed tomographic anatomy of the equine stifle joint. *Am J Vet Res*. 2011;72:512-521.
38. Crijns C, Gielen I, Van Bree H, Bergmann E. The use of CT and CT arthrography in diagnosing equine stifle injury in a Rheinlander gelding. *Equine Vet J*. 2010;42:367-371.
39. Desjardins MR, Hurtig MB. Diagnosis of equine stifle joint disorders: three cases. *Can Vet J*. 1991;32:543-550.
40. William Moyer, John Schumacher, Schumacher J: Equine joint injection and regional anesthesia. 2011.
41. Holcombe SJ, Bertone AL, Biller DS, Haider V. Magnetic resonance imaging of the equine stifle. *Vet Radiol Ultrasound*. 1995;36:119-125.
42. Naraghi A, White LM. MR imaging of cruciate ligaments. *J Magn Reson Imaging*. 2014;22:557-580.
43. Oei EH, Nikken JJ, Verstijnen AC, Ginai AZ, Hunink MG. MR imaging of the menisci and cruciate ligaments: a systematic review. *Radiology*. 2003;226:837-848.
44. Hong SH, Choi J-Y, Lee GK, Choi J-A, Chung HW, Kang HS. Grading of anterior cruciate ligament injury: diagnostic efficacy of oblique coronal magnetic resonance imaging of the knee. *J Comput Assist Tomogr*. 2003;27:814-819.
45. Umans H, Wimpfheimer O, Haramati N, Applbaum YH, Adler M, Bosco J. Diagnosis of partial tears of the anterior cruciate ligament of the knee: value of MR imaging. *AJR Am J Roentgenol*. 1995;165:893-897.
46. Samii VF, Dyce J, Pozzi A, et al. Computed tomographic arthrography of the stifle for detection of cranial and caudal cruciate ligament and meniscal tears in dogs. *Vet Radiol Ultrasound*. 2009;50:144-150.

47. Franklin SP, Cook JL, Cook CR, Shaikh LS, Clarke KM, Holmes SP. Comparison of ultrasonography and magnetic resonance imaging to arthroscopy for diagnosing medial meniscal lesions in dogs with cranial cruciate ligament deficiency. *J Am Vet Med Assoc*. 2017;251:71-79.
48. Fazio CG, Muir P, Schaefer SL, Waller KR. Accuracy of 3 tesla magnetic resonance imaging using detection of fiber loss and a visual analog scale for diagnosing partial and complete cranial cruciate ligament ruptures in dogs. *Vet Radiol Ultrasound*. 2018;59:64-78.

How to cite this article: Aßmann AD, Ohlerth S, Suárez Sánchez-Andráde J, Torgerson PR, Bischofberger AS. Ex vivo comparison of 3 Tesla magnetic resonance imaging and multidetector computed tomography arthrography to identify artificial soft tissue lesions in equine stifles. *Veterinary Surgery*. 2022;51(4):648-657. doi:10.1111/vsu.13798